



N-terminal half of transportin SR2 interacts with HIV integrase

Received for publication, January 19, 2017, and in revised form, March 14, 2017. Published, Papers in Press, March 29, 2017, DOI 10.1074/jbc.M117.777029

✉ Vicky G. Tsirkone[‡], Jolien Blokken[§], Flore De Wit[§], Jolien Breemans[‡], Stéphanie De Houwer[§], ✉ Zeger Debysers[§], Frauke Christ[§], and ✉ Sergei V. Strelkov^{‡1}

From the [‡]Laboratory for Biocrystallography and the [§]Laboratory for Molecular Virology and Gene Therapy, KU Leuven, 3000 Leuven, Belgium

Edited by Charles E. Samuel

The karyopherin transportin SR2 (TRN-SR2, TNPO3) is responsible for shuttling specific cargoes such as serine/arginine-rich splicing factors from the cytoplasm to the nucleus. This protein plays a key role in HIV infection by facilitating the nuclear import of the pre-integration complex (PIC) that contains the viral DNA as well as several cellular and HIV proteins, including the integrase. The process of nuclear import is considered to be the bottleneck of the viral replication cycle and therefore represents a promising target for anti-HIV drug design. Previous studies have demonstrated that the direct interaction between TRN-SR2 and HIV integrase predominantly involves the catalytic core domain (CCD) and the C-terminal domain (CTD) of the integrase. We aimed at providing a detailed molecular view of this interaction through a biochemical characterization of the respective protein complex. Size-exclusion chromatography was used to characterize the interaction of TRN-SR2 with a truncated variant of the HIV-1 integrase, including both the CCD and CTD. These experiments indicate that one TRN-SR2 molecule can specifically bind one CCD-CTD dimer. Next, the regions of the solenoid-like TRN-SR2 molecule that are involved in the interaction with integrase were identified using AlphaScreen binding assays, revealing that the integrase interacts with the N-terminal half of TRN-SR2 principally through the HEAT repeats 4, 10, and 11. Combining these results with small-angle X-ray scattering data for the complex of TRN-SR2 with truncated integrase, we propose a molecular model of the complex. We speculate that nuclear import of the PIC may proceed concurrently with the normal nuclear transport.

During the last decades our understanding of HIV infection has considerably increased, and a wide range of drugs targeting different steps of the viral replication cycle has been developed. However, the current combination anti-retroviral therapy has significant limitations such as the inability to completely eradicate the virus, the emergence of drug-resistant strains, adverse effects, and high cost. For these reasons, the development of new anti-HIV drugs is still necessary (1).

This work was supported by Research Foundation Flanders (FWO) Grant G0665.12 (to S. V. S. and F. C.). The authors declare that they have no conflicts of interest with the contents of this article.

¹ To whom correspondence should be addressed: Herestraat 49 bus 822, 3000 Leuven, Belgium. Tel.: 32-16330845; Fax: 32-16330764; E-mail: sergei.strelkov@kuleuven.be.

HIV, a member of the superfamily Retroviridae, can infect both dividing and non-dividing cells (2). Unlike other retroviruses, such as Gammaretroviruses, which make use of mitosis to gain access to chromatin, HIV enters the nucleus in the form of the pre-integration complex (PIC)² by means of an active transport through the nuclear pore (3). The PIC contains several components, including the reverse-transcribed viral genome, a number of viral proteins such as matrix, nucleocapsid, capsid, viral protein R, and integrase (IN), as well as cellular co-factors. Activity of IN is essential for the proliferation of the virus, as this enzyme catalyzes the irreversible incorporation of the viral DNA into the host genome. IN belongs to the superfamily of DDE(D) nucleotidyltransferases (4). The enzyme contains three domains, the N-terminal domain, the catalytic core domain (CCD), and the C-terminal domain (CTD), all implicated in multimerization that is essential for the integration process. IN recognizes the blunt ends of the linearized double-stranded and reverse-transcribed viral DNA, resulting in a complex called the intasome (5). Apart from viral proteins, cellular proteins such as the barrier to autointegration factor 1 (BAF1), high-mobility group proteins, lamina-associated polypeptide 2 α (LAP2 α), and lens epithelium-derived growth factor (LEDGF/p75) have been reported to be components of the PIC (6).

Recently, intensive research has shed more light on the HIV nuclear import. Several host factors, including import factors such as importin 7 (7), TRN-SR2 (8–11), and importin α 3 (12), as well as nucleoporins Nup153 (13) and Nup358 (14), have been proposed to be involved in this process. In addition to this complexity, intact and functional PICs are refractive to isolation and therefore revoke themselves from being studied in *in vitro* import assays. Hence, HIV nuclear import remains a highly debated topic (9, 15–20).

Both genome-wide siRNA screening as well as cell culture studies have identified TRN-SR2 as a co-factor of HIV replication, whereas the interaction between TRN-SR2 and HIV IN has been initially revealed through yeast two-hybrid studies (8, 10, 11). Subsequently, a range of experiments has indicated that TRN-SR2 is able to bind HIV integrase directly (8, 15, 21–24).

² The abbreviations used are: PIC, pre-integration complex; CTD, C-terminal domain; CCD, catalytic core domain; PDB, Protein Data Bank; SAXS, small-angle X-ray scattering; SEC, size-exclusion chromatography; HEAT, Huntington, Elongation Factor 3, PR65/A, TOR; Ni²⁺-NTA, Ni²⁺-nitrilotriacetic acid; IN, integrase; SUMO, small ubiquitin-like modifier.

Interaction of TRN-SR2 with HIV integrase

In addition, alternative hypotheses exist that postulate that TRN-SR2 engages in either direct (25, 26) or indirect interaction with a capsid protein (20, 27, 28) upon the involvement of the polyadenylation specificity factor 6 (CPSF6) in the latter case.

TRN-SR2 is a karyopherin that belongs to the importin- β family and imports mostly serine/arginine (SR)-rich splicing factors to the nucleus, including the alternative splicing factor 1/pre-mRNA-splicing factor SF2 (ASF/SF2) and cleavage and polyadenylation-specific factor (CPSF6) (29, 30). In addition, TRN-SR2 can also bind some non-SR proteins such as the RNA-binding motif protein 4 (RBM4) (31). TRN-SR2 consists of 20 consecutive Huntington, Elongation Factor 3, PR65/A, TOR (HEAT) repeats. Each repeat corresponds to two α -helices (denoted as helix *a* and helix *b*) connected by a loop and forming an α -hairpin (32, 33). Structural studies of TRN-SR2 and other importins have revealed a characteristic solenoid-like overall structure of the molecule (28, 34–37). Within each HEAT, the helix *a* is located on the outside and helix *b* on the inside of the solenoid.

It has been established that TRN-SR2 binds the substrate in the cytoplasmic compartment and subsequently docks to the nuclear pore complex, which enables its transport across the nuclear envelope. Nup358, a pivotal component of the nuclear pore complex located at the cytoplasmic side, has recently been attributed a role in transportin-mediated nuclear import (38). Once the TRN-SR2-based cargo complex reaches the nucleus, it interacts with Ras-related nuclear protein (Ran), the main regulatory co-factor of this machinery. A high nuclear concentration of RanGTP is maintained by the regulator of chromosome condensation 1 (RCC1) and the nuclear transport factor 2 (NTF2). The competitive binding of GTP-charged Ran induces cargo release (34). Previous mutagenesis and structural studies have shown that TRN-SR2 binds RanGTP via the N-terminal region, whereas the cargo attachment typically requires the arginine-rich helix 15*b* of TRN-SR2 (28, 37). The TRN-SR2-RanGTP complex eventually returns to the cytoplasm where the RanGTPase-activating protein (RanGAP) together with the Ran-binding protein 1 (RanBP1) lead to the GTP hydrolysis of Ran, which in turn induces its release from TRN-SR2 (39). It was shown that, just like *bona fide* cargoes, HIV IN can be displaced from TRN-SR2 upon addition of RanGTP (40).

HIV depends on host factors at all stages of its replication cycle. Although viral proteins generally mutate quickly especially due to the error-prone activity of the reverse transcriptase, the interfaces between the viral and host proteins may not change considerably because the host proteins are practically invariable. Correspondingly, drugs targeting the virus/host interactions are much less likely to induce the selection of resistant strains. Fortunately, a number of interactions between HIV components and cellular factors have been discovered recently opening up new opportunities for the development of novel classes of antiretroviral agents (10, 41–43). Detailed understanding of the interaction between HIV IN and human TRN-SR2 at the molecular level is crucial toward a rational design of drugs that would target this interaction, which could lead to potent antivirals due to the bottleneck nature of HIV nuclear import.

Despite its importance, the complex formation between HIV IN and human TRN-SR2 has not yet been characterized in detail at the biochemical level. One reason is that the full-length IN progressively oligomerizes in solution to a variable extent (44, 45), complicating quantitative *in vitro* studies. However, it was established previously that the interaction between TRN-SR2 and IN predominantly occurs via the CCD and CTD domains of the latter (21). Accordingly, next to the full-length protein, in this study we have employed an N-terminal truncation variant of integrase that includes the CCD and CTD domains. This variant forms dimers in solution (46). We have exploited size-exclusion chromatography (SEC) to investigate the interaction of TRN-SR2 with the CCD-CTD tandem and established the stoichiometry of the resulting complex. To pinpoint the specific interaction sites, we have used AlphaScreen binding assays involving the integrase and different truncated constructs of TRN-SR2 as well as short helical peptides thereof. Finally, we have employed small angle X-ray scattering (SAXS) to analyze the interaction between TRN-SR2 and IN in solution, which has yielded a 3D model of this molecular complex.

Results

TRN-SR2 forms a stable complex with the CCD-CTD construct of HIV-1 integrase at a 1:2 molar ratio

We used an efficient expression and purification scheme based on producing the proteins of interest as His₆-tagged small ubiquitin-like modifier (SUMO) fusions (47), followed by subtractive immobilized metal ion affinity chromatography and removal of the purification tag. Samples of highly pure recombinant human TRN-SR2 (103.9 kDa) as well as HIV-1 IN CCD-CTD tandem (24.7 kDa) could be obtained. We then used analytical SEC to systematically analyze the formation of the respective protein complex. The TRN-SR2 sample was run alone and pre-incubated with CCD-CTD in increasing molar ratios (1:1, 1:2, and 1:3). All runs reveal a single dominant peak that is increasing in intensity and somewhat shifting to the left as more CCD-CTD is being added (Fig. 1*a*). The elution position of the main peak obtained with a 2-fold excess of CCD-CTD corresponds to ~158 kDa according to a calibration by standard proteins, which is in good agreement with the theoretical value for the 1:2 complex (153 kDa). Moreover, although the mixtures containing a 1- or 2-fold molar excess of CCD-CTD do not show additional peaks in the chromatogram, the mixture with a 3-fold excess (as well as mixtures containing yet larger quantities of CCD-CTD, data not shown) reveals a distinct second peak at ~44 kDa, which corresponds to the uncomplexed CCD-CTD dimer. In line with this, for the 1:1 and 1:2 mixtures, electrophoretic analysis of the peak fraction reveals the same mass ratios of the two proteins as input, whereas for the 1:3 mix the peak fraction still appears close to the 1:2 ratio (Fig. 1*b*). Taking these observations together, we suggest that TRN-SR2 is strongly binding CCD-CTD in a 1:2 molar ratio. With a large excess of CCD-CTD, some further weak and presumably nonspecific binding is also possible. In addition, we have used the same SEC setup to analyze the mixtures of TRN-SR2 with an IN construct, including the CTD

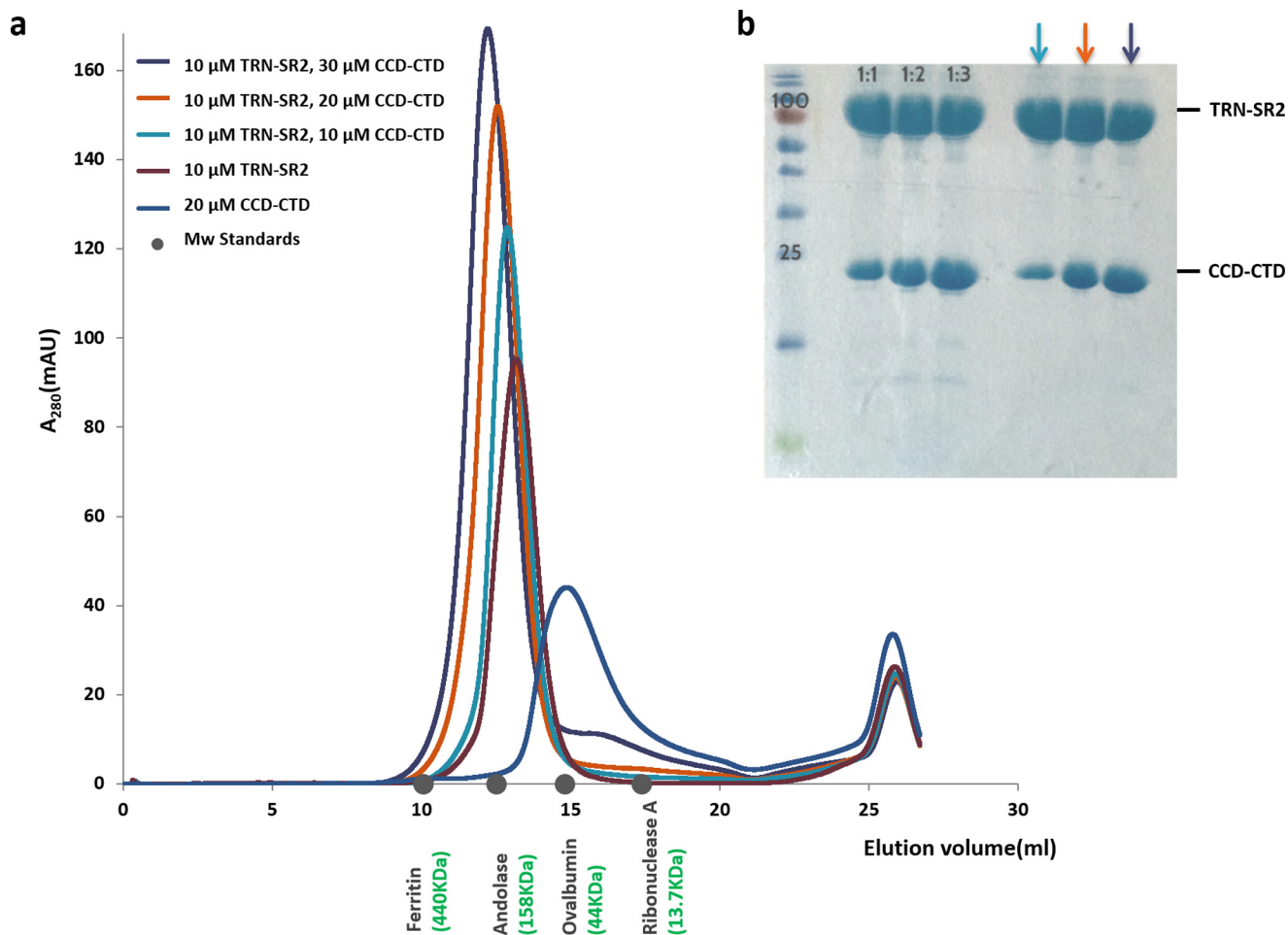


Figure 1. Complex formation between TRN-SR2 and IN CCD-CTD. *a*, size-exclusion chromatograms for TRN-SR2 incubated with CCD-CTD at 1:1, 1:2, and 1:3 molar ratios, as well as for individual proteins as indicated. Mass calibration using standard proteins is shown *below* the chromatograms. *b*, SDS-PAGE of the corresponding mixtures of TRN-SR2 and CCD-CTD, followed by the concentrated main peak fractions after the three SEC runs.

domain only. These experiments (data not shown) have confirmed also that the isolated CTD binds to TRN-SR2.

HIV-1 IN mainly binds to the N-terminal half of TRN-SR2

Previous studies have shown that the interaction between TRN-SR2 and IN predominantly occurs via the CTD of integrase, although the CCD is involved to a lesser extent (21). However, it remained obscure which parts of TRN-SR2 are responsible for the interaction with IN. Here, we have used the AlphaScreen methodology to systematically address this question.

For the initial mapping, we have prepared three consecutive fragments of TRN-SR2 each corresponding to roughly one-third of the solenoid-like molecule's length. These fragments are composed of residues 1–281, *i.e.* HEATs 1–6 and the first helix of HEAT 7 (helix 7*a*), residues 281–531, *i.e.* helix 7*b* and HEATs 8–12, and residues 531–923, *i.e.* HEATs 13–20, respectively. The two former fragments include the regions involved in the binding of RanGTP (37), whereas the third fragment includes the SR-binding helix (residues 657–671), corresponding to helix 15*b* (28). These three TRN-SR2 fragments, each carrying an N-terminal His₆ tag, were tested for interaction with IN carrying an N-terminal GST tag (Fig. 2). The full-length protein and fragments 1–281 and 281–531 displayed affinity

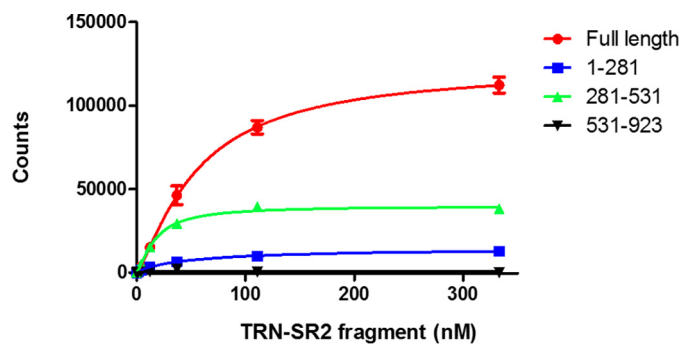


Figure 2. Interaction of full-length IN with TRN-SR2 and its fragments. AlphaScreen assays have been performed using GST-tagged integrase and His₆-tagged TRN-SR2 constructs (full-length and fragments 1–281, 281–531, and 531–923).

for IN (with apparent K_d of 17 ± 4 , 53 ± 14 , and 17 ± 1 nM, respectively), whereas the 531–923 construct did not bind to IN.

To obtain further insight into the regions involved, shorter fragments of TRN-SR2 corresponding to a single inside helix (helix *b*) from each of the 20 HEAT repeats have been prepared (except for helix 2*b* which could not be purified). These TRN-SR2 fragments were subjected to AlphaScreen assays with the full-length IN (Fig. 3, *a–c*). The same experiments were

Interaction of TRN-SR2 with HIV integrase

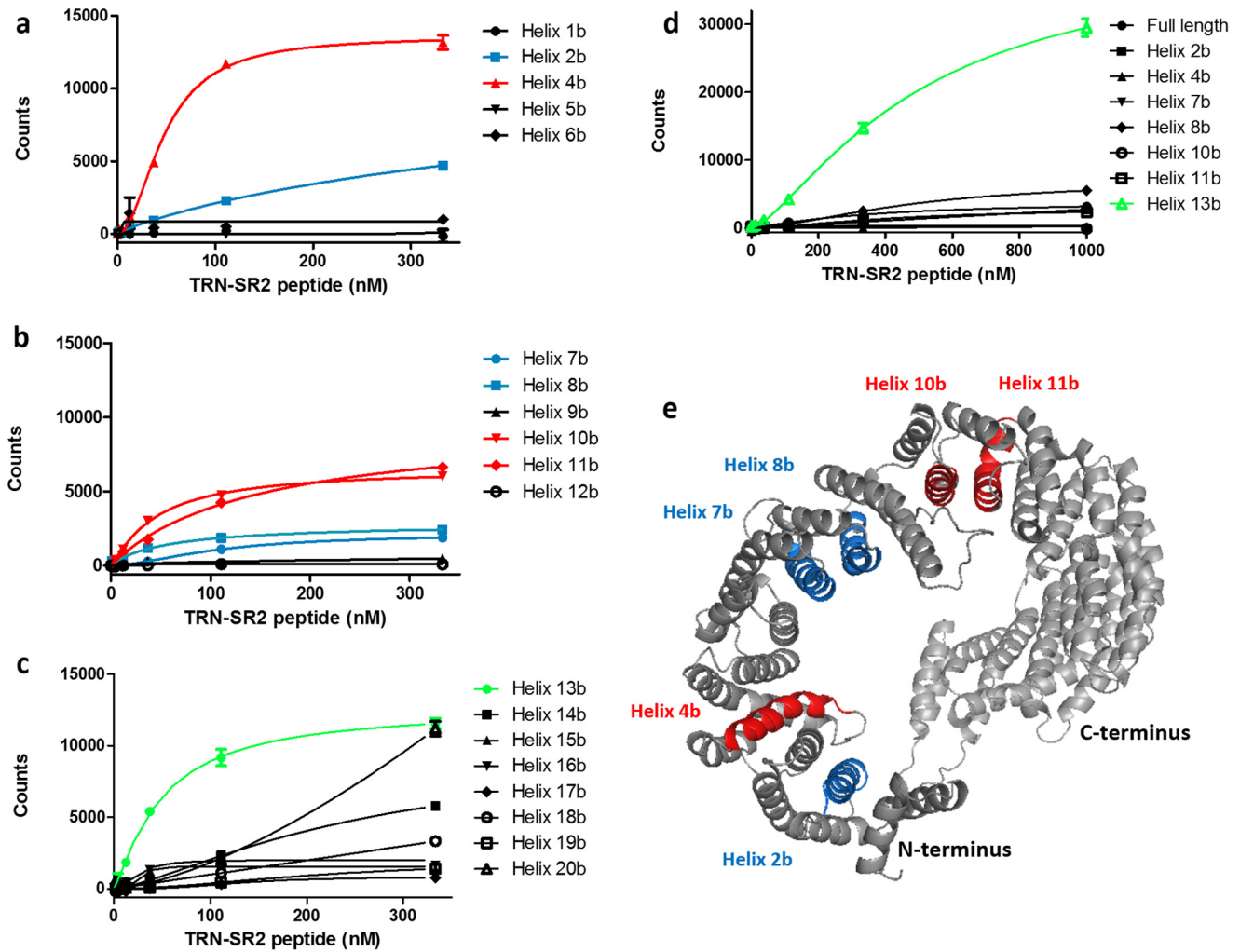


Figure 3. Interaction of full-length IN with TRN-SR2 peptides. *a–c*, AlphaScreen assays involving inner helices (as labeled) belonging to the 1–281, 281–531, and 531–923 regions, respectively. *d*, control experiment involving selected TRN-SR2 helices and LEDGF/p75, which does not bind specifically to TRN-SR2. *e*, position of the peptides interacting with IN on the three-dimensional structure (ribbon) of TRN-SR2 (PDB entry 4C0P). The TRN-SR2 peptides showing strong positive interaction with IN are colored red. The peptides showing modest interaction with IN are colored blue. Non-interacting and aspecific binders are depicted in gray.

repeated with the CCD-CTD construct, yielding essentially the same result (data not shown). To check for aspecific binding, all TRN-SR2 peptides that had tested positive to binding IN were additionally used in control experiments with LEDGF/p75, which does not bind TRN-SR2. This control experiment (Fig. 3*d*) was important because of the modest length of the peptides. As a result, a reliable, specific interaction with integrase could be established for three peptides corresponding to TRN-SR2 helices 4*b*, 10*b*, and 11*b* (Fig. 3*e*). In addition, helices 2*b*, 7*b*, and 8*b* showed some weak binding to IN. For the peptide corresponding to helix 13*b*, a clear signal was obtained with both IN and LEDGF/p75 suggesting aspecific binding. Finally, in line with the results obtained with fragment 531–923 of TRN-SR2, no binding to IN could be detected for the C-terminal helices 14*b* through 20*b*.

Thus AlphaScreen assays involving both the “one-third” constructs of TRN-SR2 and individual inside helices of each HEAT consistently indicate that the binding of IN occurs within the N-terminal half of TRN-SR2. Importantly, we have previously established that the same region of TRN-SR2 is involved in the

complex formation with RanGTP (37). Because RanGTP effectively displaces full-length IN from TRN-SR2 (40), we conclude that RanGTP directly competes with HIV IN for binding to TRN-SR2. In addition, we have carried out further out-competition experiments with integrase fragments, including CCD-CTD and also isolated CTD. Also, these two fragments were readily displaced by RanGTP (Fig. 4), confirming our hypothesis.

Structural characterization of the molecular complex between TRN-SR2 and the CCD-CTD

Attempts to crystallize TRN-SR2 in complex with HIV integrase or fragments thereof have been undertaken previously, by us and others, without success. Instead, we have resorted to SAXS experiments that can provide information about the overall structure of the macromolecular complex in a native solution environment (48, 49). Thus, we have compared the solution structure of the TRN-SR2-CCD-CTD complex and two other TRN-SR2-based protein complexes that have been previously resolved using X-ray crystallography, namely those

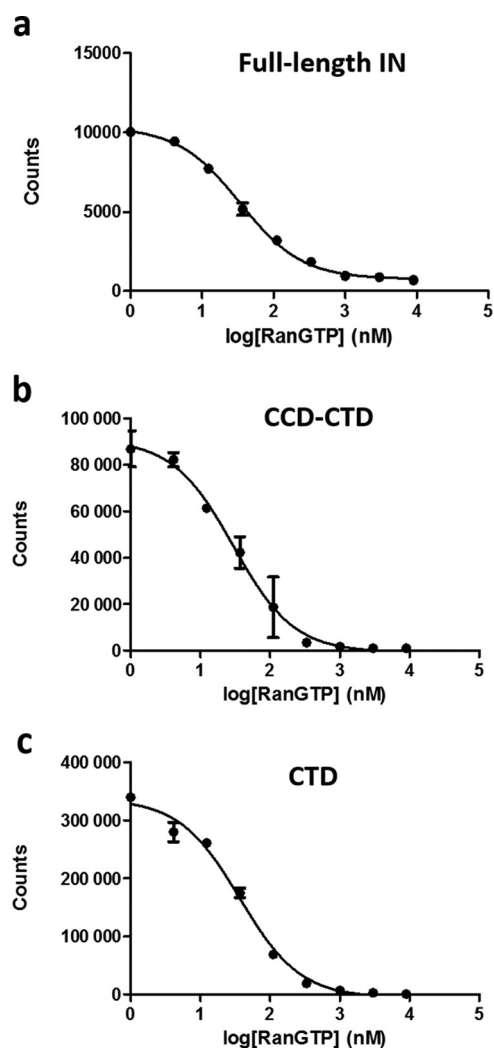


Figure 4. AlphaScreen competition assays. Full-length His₆-IN (a), His₆-CCD-CTD (b), and His₆-CTD (c) were dissociated from GST-TRN-SR2 by increasing amounts of RanGTP.

with RanGTP (37) and with a fragment of ASF/SF2 (28), an important natural cargo of TRN-SR2 (29, 50, 51). The latter fragment contained residues 106–230 of ASF/SF2, which corresponds to the second RNA recognition motif (RRM2) and a nuclear localization signal enriched in arginine and serine residues, the so-called RS domain.

Initially, the samples were subjected to SEC-SAXS analysis. Specifically, the samples were run through a SEC column, and the eluent was continuously analyzed using a synchrotron-based SAXS setup. In each case, the elution profile revealed a single main peak for the complex. Analysis of the SAXS curves for each complex yielded an essentially constant radius of gyration (R_g) value across the peak, suggesting a homogeneous sample (Fig. 5). The R_g value at the peak of the TRN-SR2·CCD-CTD complex was 45.9 Å. In contrast, both the RanGTP and ASF/SF2 complexes revealed clearly smaller R_g values (33.7 and 35.3 Å, respectively). At the same time, the expected masses of the three complexes are similar (152.7 kDa for the 1:2 complex of TRN-SR2 with CCD-CTD, 128.4 kDa for the 1:1 complex with RanGTP, and 131.7 kDa for the 1:1 complex with the ASF/SF2 fragment). These data indicate that the TRN-SR2·CCD-CTD

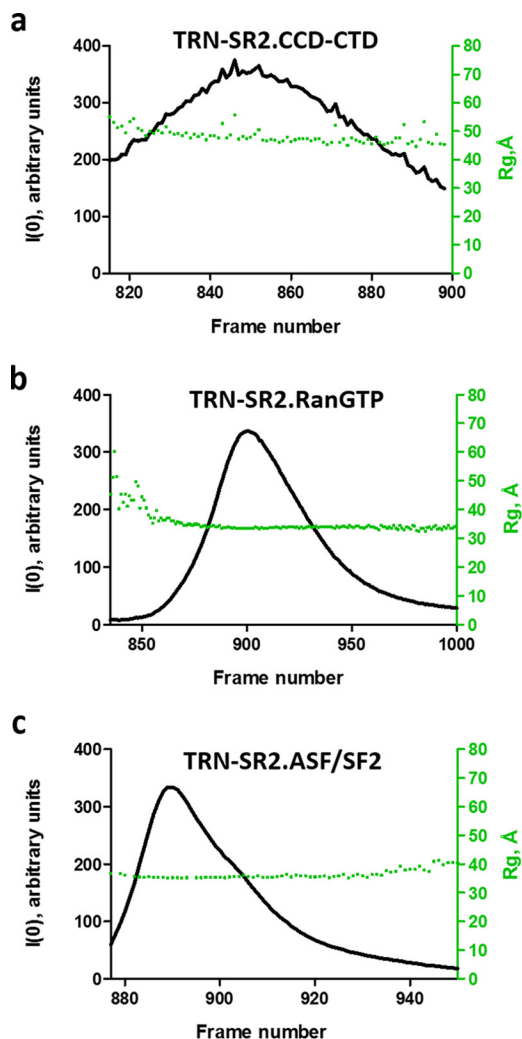


Figure 5. SEC-SAXS analysis of TRN-SR2 complexes. Plots of zero-angle scattering $I(0)$ and R_g for SAXS frames corresponding to the main elution peak, for TRN-SR2·CCD-CTD complex (a), TRN-SR2·RanGTP (b), and TRN-SR2·ASF/SF2 (c) complexes.

complex is considerably less compact than the other two complexes, because the volume characteristics are proportional to the third power of R_g .

SAXS data for TRN-SR2 complexes with both CCD-CTD and RanGTP were also collected in batch mode using a concentration series. The obtained curves for the TRN-SR2·CCD-CTD complex show some increase of the low-angle signal with increasing protein concentration but perfectly overlap at intermediate and high angles (Fig. 6a). This indicates that this complex is prone to a mild self-association, in contrast to the ideally behaving TRN-SR2·RanGTP complex (Fig. 6b) (40), whereas both complexes are quite homogeneous. We have further used five alternative SAXS-based calculations to estimate the molecular weight of the TRN-SR2·CCD-CTD complex (Table 1, see also “Experimental procedures”). All estimates, in particular the one obtained through the recently proposed method of Rambo and Tainer (52) (158.6 kDa), match well the expected mass for the 1:2 complex (152.7 kDa). This confirms the stoichiometry obtained using SEC, because the addition or removal of even a single CCD-CTD monomer would change the mass considerably (by 24.7 kDa).

Interaction of TRN-SR2 with HIV integrase

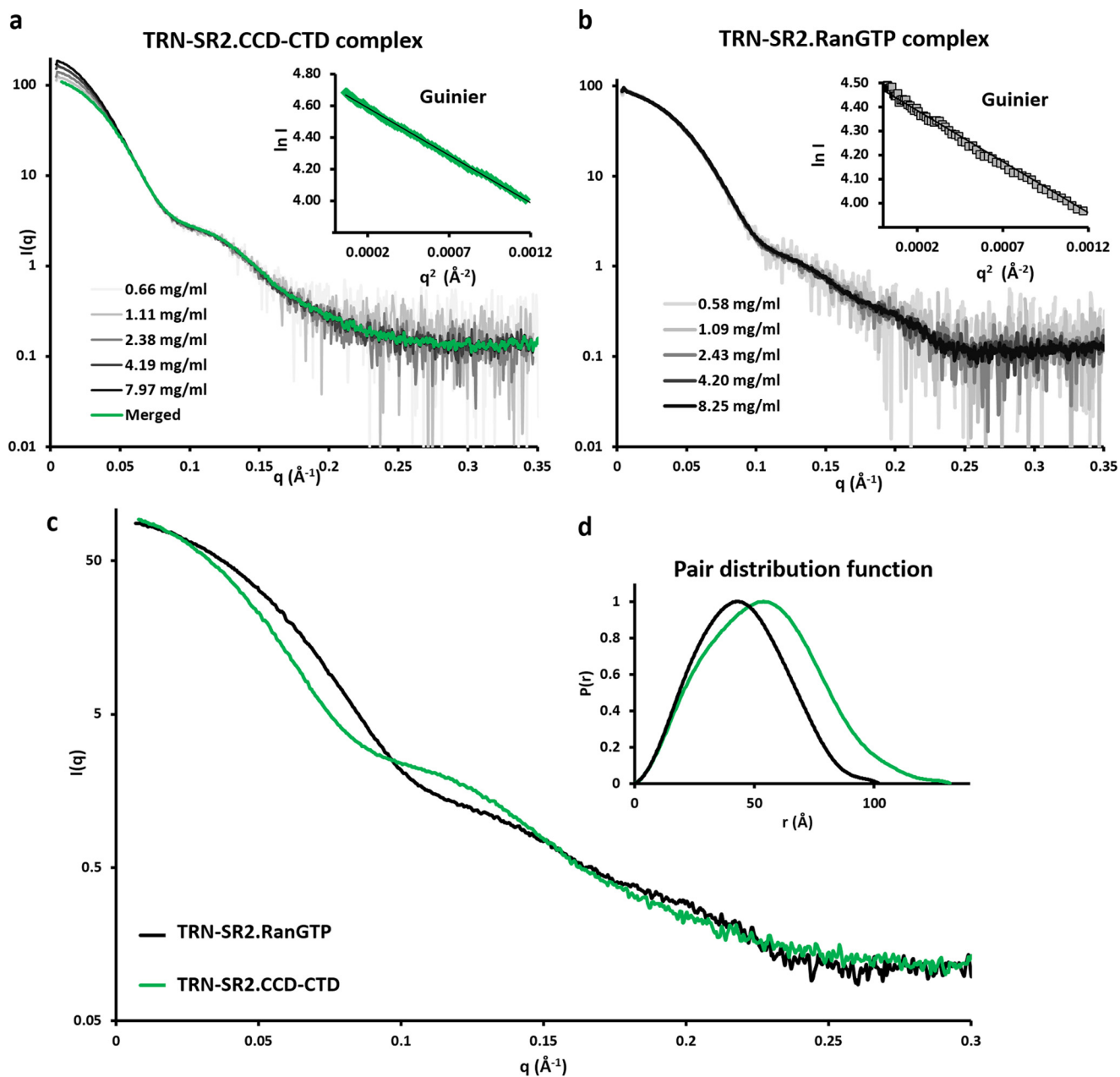


Figure 6. Detailed analysis of TRN-SR2 complexes with CCD-CTD and RanGTP using batch mode SAXS. *a*, experimental scattering curves for TRN-SR2-CCD-CTD complex in increasing concentrations (gradient of gray) and the merged curve approximating infinite dilution (green). *Inset*, Guinier plot for the latter curve. *b*, same for the TRN-SR2-RanGTP complex, with the infinite dilution approximation shown by a thick black line. *c*, superposition of the infinite dilution scattering data for both complexes. *d*, calculated pair distance distribution plots for both complexes.

The batch mode SAXS curves for the TRN-SR2·CCD-CTD and TRN-SR2·RanGTP complexes (Fig. 6c) are noticeably different, suggesting distinct overall structures of the complexes. Also, the pair distance distribution function (Fig. 6d) again suggests that the TRN-SR2 complex with CCD-CTD is considerably more extended. The maximal dimension of the TRN-SR2·CCD-CTD complex is 132 Å compared with only 102 Å for the TRN-SR2·RanGTP complex (Fig. 6d).

Finally, we have used all available structural information to create an initial model of the TRN-SR2·CCD-CTD complex, and we then further refined it using the obtained SAXS data (Fig. 7a). To this end, crystal structures of free TRN-SR2 (PDB code 4C0P) and CCD-CTD dimer (PDB code 1EX4) were first

manually docked together as rigid bodies using the molecular contact information from AlphaScreen and mutagenesis experiments. In integrase, two sets of residues have been previously identified as being important for the interaction with TRN-SR2: Phe-185/Lys-186/Arg-187/Lys-188 in the CCD and Arg-262/Arg-263/Lys-264/Lys-266/Arg-269 in the CTD (21). In TRN-SR2, the contacts with CCD-CTD were revealed by our AlphaScreen assays. A further elastic deformation (“opening”) of the TRN-SR2 solenoid was necessary to obtain a good fit between the theoretical scattering calculated from the final model and experimental SAXS data ($\chi^2 = 1.4$, Fig. 7a), which is logical given the observed increase in the maximal particle dimension. The final structural model also superimposes well

Table 1
SAXS data analysis

	TRN-SR2-CCD-CTD	TRN-SR2-RanGTP
Structural parameters		
$I(0)$ (arbitrary units) from Guinier extrapolation	110.5 ± 0.2	85.1 ± 0.2
$I(0)$ (arbitrary units) from distance distribution $P(r)$	108.6 ± 0.2	82.7 ± 0.2
R_g (Å) from Guinier	42.6 ± 1.0	35.0 ± 0.2
R_g (Å) from $P(r)$	41.3 ± 0.2	34.0 ± 0.6
Maximal dimension D_{\max} (Å)	132	102
Molecular mass determination (kDa)		
Estimated from $I(0)$ ratio with TRN-SR2-RanGTP complex	166.8	
Using SaxsMOW (67)	175.2	132.4
From Porod volume ($V_p/1.7$)	146.8	117.8
From excluded volume ($V_{ex}/1.7$)	168.6	128.9
Using volume of correlation and R_g (52)	158.6	
Expected true mass from sequence	152.7 (1:2 complex)	128.4 (1:1 complex)

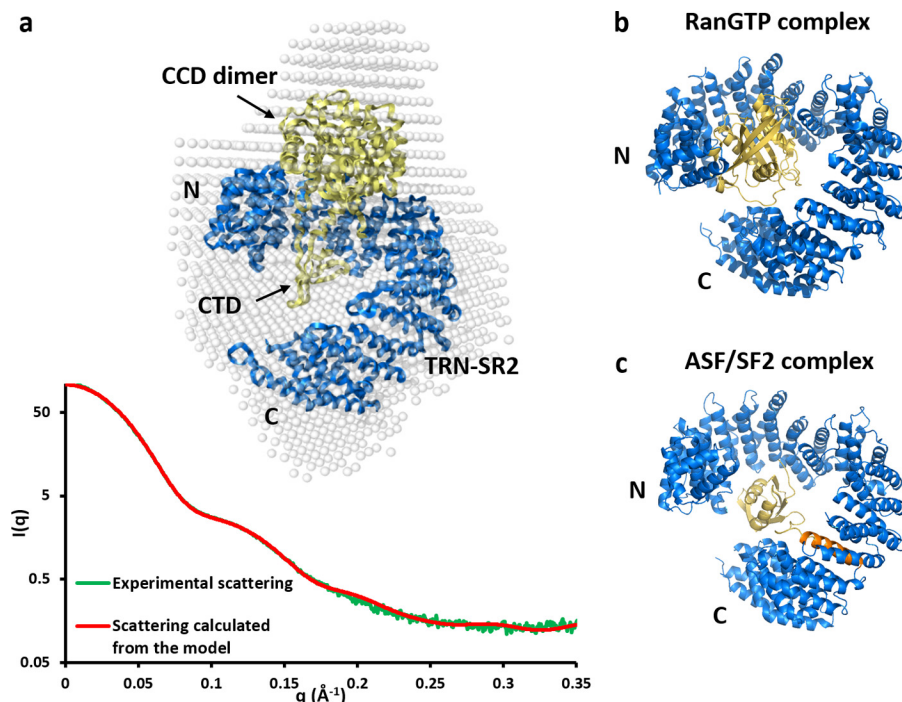


Figure 7. Three-dimensional model for the TRN-SR2-CCD-CTD complex compared with other TRN-SR2 complexes. *a*, SAXS-based model (ribbon diagram) of the CCD-CTD complex. TRN-SR2 is shown in marine. The CCD-CTD dimer is shown in yellow. The model is superimposed with the low-resolution *ab initio* shape calculated using program DAMMIN (averaged, white balls). The fit between the scattering curve calculated from the final atomic model (red) and the experimental data (green) is shown below. *b*, crystal structure of the TRN-SR2-RanGTP complex (PDB entry 4OL0), with Ran molecule in yellow, drawn to scale with the CCD-CTD complex in the previous panel. *c*, crystal structure of the TRN-SR2-ASF/SF2 fragment complex (PDB entry 4C00), drawn to scale. ASF/SF2 is in yellow. The arginine-rich helix 15*b* of TRN-SR2 critical to the binding is highlighted in orange.

with the *ab initio* molecular envelope obtained directly from the SAXS data (Fig. 7*a*).

Discussion

By now, TRN-SR2 is widely accepted as a key player in HIV nuclear import. However, the exact mechanism of its involvement is a subject of ongoing debate. Here, we have demonstrated a direct interaction between recombinant, highly purified samples of both human TRN-SR2 and HIV-1 IN, and we performed a systematic *in vitro* characterization of the resulting macromolecular complex using a range of biochemical and structural methods.

Titration of TRN-SR2 with increasing amounts of the CCD-CTD fragment of HIV integrase followed by SEC runs revealed a 1:2 stoichiometry for the primary binding (Fig. 1). This correlates well with the fact that the CCD-CTD dimerizes via the

CCD (46). It is logical to suggest that the dimeric state of CCD-CTD is preserved upon its engagement in a complex with TRN-SR2. At the same time, it is the CTD of integrase that is known to provide the main contribution toward binding to TRN-SR2 (21, 53, 54). Interestingly, isolated CTD dimerizes in solution (55), and such CTD dimers could be observed in the recently published structure of the HIV-1 intasome (56).

We have also investigated which parts of TRN-SR2 are responsible for the interaction with HIV IN. Using AlphaScreen methodology, we could establish that IN binds to two fragments of TRN-SR2 each corresponding to about one-third of the total solenoid-like molecule, namely the fragments comprising residues 1–281 (*i.e.* HEATS 1–7) and 281–531 (*i.e.* HEATS 7–12), respectively, whereas the remaining C-terminal fragment did not bind the IN. We have further delineated three individual peptides, corre-

Interaction of TRN-SR2 with HIV integrase

sponding to the inner α -helices of HEAT repeats 4, 10, and 11, as strong IN binders. These data indicate that HIV integrase mainly interacts with TRN-SR2 through its N-terminal half (up to and including HEAT 11).

The final component of this work was the study of the TRN-SR2-CCD-CTD complex in solution using SAXS, a technique that had been previously employed to characterize both the uncomplexed TRN-SR2 (54) and the TRN-SR2-RanGTP complex (40). As a result, we could derive a SAXS-based 3D model of the TRN-SR2-CCD-CTD complex. It is interesting to compare this model with the available crystal structures of TRN-SR2 complexes with RanGTP and ASF/SF2 (Fig. 7) (28, 37).

Generally speaking, binding within the N-terminal half of TRN-SR2 that we have observed here for the HIV IN CCD-CTD appears to be a recurring feature for various interacting partners. In TRN-SR2 complex with RanGTP, the latter was shown to be interacting mainly with the HEAT repeats 1–9 but also reaching to the C terminus, in particular HEAT 18 (Fig. 7*b*) (37). The crystal structure with the ASF/SF2 fragment (residues 106–230) (28) revealed binding of the RRM2 domain mainly to HEAT repeats 4–7, with some involvement of the C-terminal HEATs 19 and 20. In addition, the phosphorylated RS domain was binding to HEATs 14–17, which in particular includes the arginine-rich helix 15*b* (Fig. 7*c*).

In this respect, it not surprising that the full-length IN but also its CCD-CTD fragment and isolated CTD domain were readily expelled from the complex with TRN-SR2 upon RanGTP addition (Fig. 4). This process resembles the action of RanGTP on TRN-SR2-bound natural cargoes. At the same time, the described motif of IN interaction with TRN-SR2 appears to leave the helix 15*b* of the latter accessible to binding the RS motif of *bona fide* partners such as ASF/SF2. Previously, a TRN-SR2 mutant carrying multiple alanine mutations of residues involved in binding the RS motif was shown to bind IN equally efficiently as the wild-type TRN-SR2 (28). As a future possibility, point mutagenesis within the HEAT repeats 4, 10, and 11 shown here to interact with IN would help to delineate the specific interacting amino acids in TRN-SR2. However, a statistically rigorous scanning would require testing a large number of alanine mutations.

The solenoid-like TRN-SR2 molecule appears to be rather flexible. Previously, high-resolution X-ray crystallographic studies have revealed that tight intermolecular interactions make the solenoid-like TRN-SR2 wrap around either the ASF/SF2 fragment or RanGTP, reducing the radius of gyration of the complex compared with free TRN-SR2 (28, 37). At the same time, our new SAXS data reveal that the TRN-SR2-CCD-CTD complex is, by contrast, considerably less compact than the complexes of TRN-SR2 with either the ASF/SF2 fragment or RanGTP, as evidenced by an $\sim 30\%$ increase in the radius of gyration. This difference is also apparent from a side-by-side comparison of the respective molecular models (Fig. 7). Apparently, the weaker interaction of TRN-SR2 with CCD-CTD is leading to a more open solenoid structure of TRN-SR2, which is the dominant component of the complex.

Several studies of the intasome, the complex of IN and viral DNA, are available. A crystal structure of the prototype foamy virus intasome has revealed a tetramer of IN bound to DNA,

which is the minimal functional state required for a concerted integration (57). A crystal structure of the Rous sarcoma virus intasome (58) and a cryo-EM structure of mouse mammary tumor virus intasome (59) showed the existence of an octameric state, whereas a cryo-EM structure of maedi-visna lentivirus intasome presented a tetramer-of-tetramers architecture (60). Most recently, by fusing the DNA-binding protein Sso7d to the N terminus of HIV-1 integrase, it became possible to obtain a sample suitable for cryo-EM, yielding the first 3D structure of the HIV-1 intasome, including four IN chains (56).

Thus, although the HIV-1 particles contain ~ 250 copies of IN, only four of them appear to be involved in the intasome. Other IN chains may be expected to have a structural role within the PIC and/or orchestrate the nuclear import. In particular, the CTDs, which do not directly interact with the viral or target DNA but are exposed on the surface of the PIC, could interact with TRN-SR2. Moreover, our data suggest that the interaction between IN and TRN-SR2 does not involve the SR-binding region, which implies that a simultaneous transport of natural cargoes and HIV IN would be feasible, suggesting a model wherein the viral PIC is a stowaway during the TRN-SR2-mediated nuclear import of *bona fide* cargoes, such as ASF/SF2 and CPSF6. Finally, the new molecular insights into this interaction obtained here validate the interaction interface toward a rational design of compounds with inhibitory effect. Such lead compounds have a potential of becoming a future class of antiretroviral agents.

Experimental procedures

Expression and purification of proteins for biochemical and SAXS studies

Full-length human TRN-SR2 was inserted into the pETH-SUK vector, a derivative of pETHSUL (47), using the In-Fusion system (Clontech) essentially as described previously (37). The expressed fusion product contained an N-terminal His₆ tag, the SUMO protein, a SUMO hydrolase cleavage site, and the TRN-SR2 sequence. The protein was overexpressed in *Escherichia coli* NICO21 (DE3) strain (New England Biolabs) containing the pRARE2 plasmid (EMD Biosciences). Bacterial cultures were grown in ZYP-5052 autoinduction media at 24 °C until $A_{600\text{ nm}}$ reached ~ 4 and then for another 24 h at 18 °C until $A_{600\text{ nm}}$ reached ~ 16 (61). The cells were pelleted by centrifugation and resuspended in buffer A (50 mM Tris-HCl, pH 7.5, 200 mM NaCl, 15 mM imidazole, 5 mM β -mercaptoethanol). After addition of 5 μ l of a cold-active nuclease Cryonase (Clontech) per 100 ml, the cells were lysed using an EmulsiFlex-C5 homogenizer (Avestin) followed by sonication on ice for 2 min with 40% amplitude and 2/2-s on/off pulses using the Branson Digital Sonifier. The lysates were cleared at $18,000 \times g$ for 35 min at 4 °C and then were applied on a Ni²⁺-NTA (GE Healthcare) column using buffer A, followed by elution with buffer B (buffer A supplemented with 500 mM imidazole). Subsequently, the tag was cleaved off by an overnight incubation with SUMO hydrolase in a 1:500 molar ratio at 4 °C in buffer A. This was followed by a second purification through the Ni²⁺-NTA column, whereby the flow-through containing the cleaved protein was collected, and the uncleaved protein and the protease, both

containing the His₆-SUMO tag, were retained on the column. The buffer was subsequently exchanged for 20 mM Tris-HCl, pH 7.5, 50 mM NaCl, 5 mM DTT using an Ultra-15 ultrafiltration device (Amicon), which was followed by ion-exchange chromatography on a 5-ml HiTrap Q HP column (GE Healthcare) using a linear gradient of 50 mM to 1 M NaCl.

The IN construct corresponding to CCD-CTD (residues 52–273) was expressed and purified similarly to methods described above for TRN-SR2. The lysates were purified with a Ni²⁺-NTA (GE Healthcare) column using buffer A in the washing step, and the protein was eluted by using buffer B, both supplemented with 1 M NaCl. SEC on a HiLoad 16/60 Superdex 200 preparation grade column (GE Healthcare) was then performed in 20 mM Tris-HCl, pH 7.5, 1 M NaCl, 5 mM DTT.

Inactive Q69L mutant of Ran protein has been overexpressed, purified, and charged with GTP as described previously (37). Thereafter the protein was incubated with TRN-SR2, and the resulting complex was purified using SEC (37).

Truncated ASF/SF2, which includes residues 106–230 corresponding to the RRM2 and RS domains, has been inserted into the pETHSUK vector and co-expressed with human CDC-like kinase 1, resulting in *in vitro* phosphorylation of ASF/SF2. The expression and purification of ASF/SF2 as well as formation and isolation of its complex with TRN-SR2 were done essentially as described previously (28).

Complex formation between TRN-SR2 and CCD-CTD and analytical SEC

The proteins were mixed in 20 mM Tris-HCl, pH 7.5, 150 mM NaCl, 5 mM DTT at different molar ratios and incubated on ice for 1 h. Thereafter, the sample (150 μ l) was applied on a Superdex 200 10/300 column (23-ml volume, GE Healthcare) in the same buffer, and the eluted fractions were analyzed on a 15% PAGE in the presence of SDS-PAGE and stained with Coomassie Blue.

AlphaScreen interaction assays

Cloning, expression, and purification of tagged protein constructs for AlphaScreen assay was done essentially as described previously (8, 62). Briefly, the pGEX expression plasmid was used as a template for cloning individual helical peptides of TRN-SR2. *E. coli* BL21-CodonPlus (DE3) cells were grown to an $A_{600\text{ nm}}$ of 0.6, and protein expression was induced with 0.5 mM isopropyl β -thiogalactopyranoside. After incubation at 37 °C for 2 h, the bacteria were harvested and then resuspended in a lysis buffer (PBS, pH 7.4, 1 M NaCl, 1 mM DTT, 1 mg/ml lysozyme, 1 mM PMSF, 1 μ l of DNase/10 ml, and 1% Triton X-100). After complete cell lysis by sonication, the supernatant was cleared by centrifugation, and recombinant proteins were bound to the glutathione-Sepharose resin (GE Healthcare). After washing the resin with 20 volumes of washing buffer (PBS, pH 7.4, 1 M NaCl, 1 mM DTT), the GST-tagged peptides were eluted with 5 ml of elution buffer (washing buffer supplied with 20 mM reduced glutathione). The fractions were analyzed using SDS-PAGE for protein content, pooled, and supplemented with 10% glycerol.

AlphaScreen assays were performed at least in duplicate as described previously (21). In the first series of experiments, GST-tagged full-length integrase at a fixed concentration of

about 80 nM was tested against increasing concentrations of His₆-tagged TRN-SR2 constructs (full-length, 1–281, 281–531, and 531–928). Protein concentrations were determined by $A_{280\text{ nm}}$. The apparent dissociation constant (K_d) was calculated assuming a simple bimolecular reaction. In the second series, His₆-tagged full-length IN and His₆-SUMO-CCD-CTD (uncleaved fusion) were tested against GST-tagged full-length TRN-SR2 as well as its individual peptides. Finally, to check for aspecific binding, all TRN-SR2 peptides that had tested positive to binding integrase were additionally used in control experiments involving His₆-tagged LEDGF/p75, obtained as described previously (63). In addition, out-competition experiments were performed using His₆-tagged integrase (full-length, CCD-CTD, or CTD) and GST-tagged TRN-SR2 and increasing concentrations of untagged RanGTP. To this end, optimal binding concentrations of IN constructs and TRN-SR2 were first determined using cross-titration experiments.

SAXS measurements

Synchrotron X-ray scattering data were collected at the beamline BM29 of European Synchrotron Radiation Facility (Grenoble, France) and the SWING beamline of Synchrotron Soleil (Paris, France). X-ray radiation wavelength (λ) of about 1 Å and a PILATUS 1M detectors were used. The data were collected up to $q = 4\pi \sin\theta/\lambda = 0.5 \text{ 1/Å}$, where 2θ is the scattering angle.

First, the samples have been subjected to SEC separation at 10 °C followed by an in-line SAXS measurement (SEC-SAXS). To this end, a Shodex KW404-4F column equilibrated with 25 mM Tris-HCl, pH 7.5, 150 mM NaCl, 10 mM DTT was used. 200 μ l of protein sample at $\sim 10 \text{ mg/ml}$ in the same buffer was injected. The eluent at 0.2 ml/min rate has been continuously analyzed by SAXS using 1-s frames. Initial processing, including radial averaging and buffer subtraction, was performed by an automatic pipeline (64). The ATSAS program package (65) and the DATASW program (66) were used for further processing.

Second, protein samples were also analyzed using a batch mode SAXS. To this end, a concentration series from ~ 0.6 to 8 mg/ml in 20 mM Tris-HCl, pH 7.5, 150 mM NaCl, and 10 mM DTT was used. No radiation damage was detected for 10 successive frames with a 2-s exposure. Comparison of the SAXS curves collected from samples at various concentrations indicated some increase of the low-angle signal with concentration for the TRN-SR2·CCD-CTD complex. Correspondingly, subsequent analysis of these complexes used a merged scattering curve that had been generated from the low-angle part of the lowest concentration curve ($\sim 0.6 \text{ mg/ml}$) and the remaining part of the highest concentration curve ($\sim 8 \text{ mg/ml}$), as an approximation of a dilute solution. The distance distribution function $P(r)$ and the Porod volume were calculated using the program GNOM from the ATSAS package. The molecular weight of the TRN-SR2·CCD-CTD complex was estimated using five different methods as follows: (i) based on the $I(0)$ value ratio compared with the TRN-SR2·RanGTP complex, using the known mass (128.4 kDa) of the latter as a reference; (ii) based on the excluded volume of the hydrated particle using the Porod invariant (65); (iii) using the excluded volume of the DAMMIN model (65); (iv) using the program SAXSMoW (67)

Interaction of TRN-SR2 with HIV integrase

that calculates the particle volume based on the experimental data regularized with GNOM; and (v) the method of Rambo and Tainer (52). *Ab initio* models without symmetry were created using low-resolution data in the range $0.011 < s < 0.24 \text{ \AA}^{-1}$ with DAMMIN (68). Ten independent runs were performed and averaged using DAMAVER (Table 1) (69).

The model of the rigid-body complex of TRN-SR2 and the CCD-CTD dimer was optimized through the program SASREF (70) using molecular contact restraints derived from mutagenesis and AlphaScreen data. When exact crystallographic conformations were used, the final fit between the scattering calculated from the model and the experimental SAXS data had a χ^2 of 3.2. Thereafter, the TRN-SR2 molecule was opened up using the normal mode elastic deformation server NOMAD-Ref (71) with amplitude corresponding to an $\sim 3\text{-\AA}$ root mean square deviation from the initial structure, and the same docking procedure with CCD-CTD dimer was repeated. This has allowed us to improve the fit to the experimental data ($\chi^2 = 2.0$). Thereafter, the program SREFLEX (72) was used to apply additional normal mode deformations, yielding the final model with $\chi^2 = 1.4$.

Author contributions—V. G. T., Z. D., F. C., and S. V. S. designed the study; V. G. T., J. Blokken, F. D. W., S. D. H., and J. Breemans performed the experiments; V. G. T., J. Blokken, and S. V. S. analyzed the data; V. G. T. and S. V. S. wrote the manuscript with help from J. Blokken, F. D. W., Z. D., and F. C. All authors approved the final version of the manuscript.

Acknowledgments—We thank Dr. Stephen D. Weeks for guidance on cloning and protein expression as well as for help with SAXS data collection and Dr. Alexander V. Shkumatov for valuable advice on SAXS data collection and processing. An expression plasmid for human CDC-like kinase 1 was a kind gift of Prof. Peter Cherepanov. Research at the Laboratory of Molecular Virology and Gene Therapy was also funded by Belgian IAP BelVir. Support from the Seventh Framework Programme of the EC under the BioStruct-X initiative (Project Number 6131) toward the synchrotron SAXS measurements is acknowledged.

References

- Engelman, A., and Cherepanov, P. (2012) The structural biology of HIV-1: mechanistic and therapeutic insights. *Nat. Rev. Microbiol.* **10**, 279–290
- Yamashita, M., and Emerman, M. (2006) Retroviral infection of non-dividing cells: old and new perspectives. *Virology* **344**, 88–93
- Lusic, M., and Siliciano, R. F. (2016) Nuclear landscape of HIV-1 infection and integration. *Nat. Rev. Microbiol.* 10.1038/nrmicro.2017.22
- Cherepanov, P., Maertens, G. N., and Hare, S. (2011) Structural insights into the retroviral DNA integration apparatus. *Curr. Opin. Struct. Biol.* **21**, 249–256
- Hare, S., Maertens, G. N., and Cherepanov, P. (2012) 3'-Processing and strand transfer catalysed by retroviral integrase *in crystallo*. *EMBO J.* **31**, 3020–3028
- Suzuki, Y., and Craigie, R. (2007) The road to chromatin–nuclear entry of retroviruses. *Nat. Rev. Microbiol.* **5**, 187–196
- Fassati, A., Görlich, D., Harrison, I., Zaytseva, L., and Mingot, J. M. (2003) Nuclear import of HIV-1 intracellular reverse transcription complexes is mediated by importin 7. *EMBO J.* **22**, 3675–3685
- Christ, F., Thys, W., De Rijck, J., Gijsbers, R., Albanese, A., Arosio, D., Emiliani, S., Rain, J. C., Benarous, R., Cereseto, A., and Debysers, Z. (2008) Transportin-SR2 imports HIV into the nucleus. *Curr. Biol.* **18**, 1192–1202
- Thys, W., De Houwer, S., Demeulemeester, J., Taltynov, O., Vancraenenbroeck, R., Gérard, M., De Rijck, J., Gijsbers, R., Christ, F., and Debysers, Z. (2011) Interplay between HIV entry and transportin-SR2 dependency. *Retrovirology* **8**, 7
- Brass, A. L., Dykxhoorn, D. M., Benita, Y., Yan, N., Engelman, A., Xavier, R. J., Lieberman, J., and Elledge, S. J. (2008) Identification of host proteins required for HIV infection through a functional genomic screen. *Science* **319**, 921–926
- König, R., Zhou, Y., Elleder, D., Diamond, T. L., Bonamy, G. M., Irelan, J. T., Chiang, C. Y., Tu, B. P., De Jesus, P. D., Lilley, C. E., Seidel, S., Opaluch, A. M., Caldwell, J. S., Weitzman, M. D., Kuhen, K. L., *et al.* (2008) Global analysis of host-pathogen interactions that regulate early-stage HIV-1 replication. *Cell* **135**, 49–60
- Ao, Z., Danappa Jayappa, K., Wang, B., Zheng, Y., Kung, S., Rassart, E., Depping, R., Kohler, M., Cohen, E. A., and Yao, X. (2010) Importin $\alpha 3$ interacts with HIV-1 integrase and contributes to HIV-1 nuclear import and replication. *J. Virol.* **84**, 8650–8663
- Woodward, C. L., Prakobwanakit, S., Mosessian, S., and Chow, S. A. (2009) Integrase interacts with nucleoporin NUP153 to mediate the nuclear import of human immunodeficiency virus type 1. *J. Virol.* **83**, 6522–6533
- Ocwieja, K. E., Brady, T. L., Ronen, K., Huegel, A., Roth, S. L., Schaller, T., James, L. C., Towers, G. J., Young, J. A., Chanda, S. K., König, R., Malani, N., Berry, C. C., and Bushman, F. D. (2011) HIV integration targeting: a pathway involving Transportin-3 and the nuclear pore protein RanBP2. *PLoS Pathog.* **7**, e1001313
- Levin, A., Hayouka, Z., Friedler, A., and Loyter, A. (2010) Transportin 3 and importin α are required for effective nuclear import of HIV-1 integrase in virus-infected cells. *Nucleus* **1**, 422–431
- Krishnan, L., Li, X., Naraharisetty, H. L., Hare, S., Cherepanov, P., and Engelman, A. (2010) Structure-based modeling of the functional HIV-1 intasome and its inhibition. *Proc. Natl. Acad. Sci. U.S.A.* **107**, 15910–15915
- Matreyek, K. A., and Engelman, A. (2013) Viral and cellular requirements for the nuclear entry of retroviral preintegration nucleoprotein complexes. *Viruses* **5**, 2483–2511
- Jayappa, K. D., Ao, Z., and Yao, X. (2012) The HIV-1 passage from cytoplasm to nucleus: the process involving a complex exchange between the components of HIV-1 and cellular machinery to access nucleus and successful integration. *Int. J. Biochem. Mol. Biol.* **3**, 70–85
- Chin, C. R., Ferreira, J. M., Savidis, G., Portmann, J. M., Aker, A. M., Feeley, E. M., Smith, M. C., and Brass, A. L. (2015) Direct visualization of HIV-1 replication intermediates shows that capsid and CPSF6 modulate HIV-1 intra-nuclear invasion and integration. *Cell Rep.* **13**, 1717–1731
- Bhattacharya, A., Alam, S. L., Fricke, T., Zadrozny, K., Sedzicki, J., Taylor, A. B., Demeler, B., Pornillos, O., Ganser-Pornillos, B. K., Diaz-Griffero, F., Ivanov, D. N., and Yeager, M. (2014) Structural basis of HIV-1 capsid recognition by PF74 and CPSF6. *Proc. Natl. Acad. Sci. U.S.A.* **111**, 18625–18630
- De Houwer, S., Demeulemeester, J., Thys, W., Taltynov, O., Zmajkovicova, K., Christ, F., and Debysers, Z. (2012) Identification of residues in the C-terminal domain of HIV-1 integrase that mediate binding to the transportin-SR2 protein. *J. Biol. Chem.* **287**, 34059–34068
- Luban, J. (2008) HIV-1 infection: going nuclear with TNPO3/Transportin-SR2 and integrase. *Curr. Biol.* **18**, R710–713
- Ao, Z., Fowke, K. R., Cohen, E. A., and Yao, X. (2005) Contribution of the C-terminal tri-lysine regions of human immunodeficiency virus type 1 integrase for efficient reverse transcription and viral DNA nuclear import. *Retrovirology* **2**, 62
- Gallay, P., Hope, T., Chin, D., and Trono, D. (1997) HIV-1 infection of nondividing cells through the recognition of integrase by the importin/karyopherin pathway. *Proc. Natl. Acad. Sci. U.S.A.* **94**, 9825–9830
- Valle-Casuso, J. C., Di Nunzio, F., Yang, Y., Reszka, N., Lienlaf, M., Arhel, N., Perez, P., Brass, A. L., and Diaz-Griffero, F. (2012) TNPO3 is required for HIV-1 replication after nuclear import but prior to integration and binds the HIV-1 core. *J. Virol.* **86**, 5931–5936
- Zhou, L., Sokolskaja, E., Jolly, C., James, W., Cowley, S. A., and Fassati, A. (2011) Transportin 3 promotes a nuclear maturation step required for efficient HIV-1 integration. *PLoS Pathog.* **7**, e1002194

27. Hori, T., Takeuchi, H., Saito, H., Sakuma, R., Inagaki, Y., and Yamaoka, S. (2013) A carboxy-terminally truncated human CPSF6 lacking residues encoded by exon 6 inhibits HIV-1 cDNA synthesis and promotes capsid disassembly. *J. Virol.* **87**, 7726–7736
28. Maertens, G. N., Cook, N. J., Wang, W., Hare, S., Gupta, S. S., Öztop, I., Lee, K., Pye, V. E., Cosnefroy, O., Snijders, A. P., KewalRamani, V. N., Fassati, A., Engelman, A., and Cherepanov, P. (2014) Structural basis for nuclear import of splicing factors by human transportin 3. *Proc. Natl. Acad. Sci. U.S.A.* **111**, 2728–2733
29. Lai, M. C., Lin, R. I., and Tarn, W. Y. (2001) Transportin-SR2 mediates nuclear import of phosphorylated SR proteins. *Proc. Natl. Acad. Sci. U.S.A.* **98**, 10154–10159
30. Lee, K., Ambrose, Z., Martin, T. D., Oztop, I., Mulky, A., Julias, J. G., Vandegraaff, N., Baumann, J. G., Wang, R., Yuen, W., Takemura, T., Shelton, K., Taniuchi, I., Li, Y., Sodroski, J., Littman, D. R., et al. (2010) Flexible use of nuclear import pathways by HIV-1. *Cell Host Microbe* **7**, 221–233
31. Lai, M. C., Kuo, H. W., Chang, W. C., and Tarn, W. Y. (2003) A novel splicing regulator shares a nuclear import pathway with SR proteins. *EMBO J.* **22**, 1359–1369
32. Andrade, M. A., and Bork, P. (1995) HEAT repeats in the Huntington's disease protein. *Nat. Genet.* **11**, 115–116
33. Groves, M. R., Hanlon, N., Turowski, P., Hemmings, B. A., and Barford, D. (1999) The structure of the protein phosphatase 2A PR65/A subunit reveals the conformation of its 15 tandemly repeated HEAT motifs. *Cell* **96**, 99–110
34. Bono, F., Cook, A. G., Grünwald, M., Ebert, J., and Conti, E. (2010) Nuclear import mechanism of the EJC component Mago-Y14 revealed by structural studies of importin 13. *Mol. Cell* **37**, 211–222
35. Vetter, I. R., Arndt, A., Kutay, U., Görlich, D., and Wittinghofer, A. (1999) Structural view of the Ran-Importin β interaction at 2.3 Å resolution. *Cell* **97**, 635–646
36. Imasaki, T., Shimizu, T., Hashimoto, H., Hidaka, Y., Kose, S., Imamoto, N., Yamada, M., and Sato, M. (2007) Structural basis for substrate recognition and dissociation by human transportin 1. *Mol. Cell* **28**, 57–67
37. Tsirkone, V. G., Beutels, K. G., Demeulemeester, J., Debyser, Z., Christ, F., and Strelkov, S. V. (2014) Structure of transportin SR2, a karyopherin involved in human disease, in complex with Ran. *Acta Crystallogr. F Struct. Biol. Commun.* **70**, 723–729
38. Hutten, S., Wälde, S., Spillner, C., Hauber, J., and Kehlenbach, R. H. (2009) The nuclear pore component Nup358 promotes transportin-dependent nuclear import. *J. Cell Sci.* **122**, 1100–1110
39. Fried, H., and Kutay, U. (2003) Nucleocytoplasmic transport: taking an inventory. *Cell. Mol. Life Sci.* **60**, 1659–1688
40. Taltynov, O., Demeulemeester, J., Christ, F., De Houwer, S., Tsirkone, V. G., Gerard, M., Weeks, S. D., Strelkov, S. V., and Debyser, Z. (2013) Interaction of transportin-SR2 with Ras-related nuclear protein (Ran) GTPase. *J. Biol. Chem.* **288**, 25603–25613
41. Christ, F., Voet, A., Marchand, A., Nicolet, S., Desimmié, B. A., Marchand, D., Bardiot, D., Van der Veken, N. J., Van Remoortel, B., Strelkov, S. V., De Maeyer, M., Chaltin, P., and Debyser, Z. (2010) Rational design of small-molecule inhibitors of the LEDGF/p75-integrase interaction and HIV replication. *Nat. Chem. Biol.* **6**, 442–448
42. Taltynov, O., Desimmié, B. A., Demeulemeester, J., Christ, F., and Debyser, Z. (2012) Cellular cofactors of lentiviral integrase: from target validation to drug discovery. *Mol. Biol. Int.* **2012**, 863405
43. Arhel, N., and Kirchhoff, F. (2010) Host proteins involved in HIV infection: new therapeutic targets. *Biochim. Biophys. Acta* **1802**, 313–321
44. Guiot, E., Carayon, K., Delelis, O., Simon, F., Tauc, P., Zubin, E., Gottikh, M., Mouscadet, J. F., Brochon, J. C., and Deprez, E. (2006) Relationship between the oligomeric status of HIV-1 integrase on DNA and enzymatic activity. *J. Biol. Chem.* **281**, 22707–22719
45. Deprez, E., Tauc, P., Leh, H., Mouscadet, J. F., Auclair, C., and Brochon, J. C. (2000) Oligomeric states of the HIV-1 integrase as measured by time-resolved fluorescence anisotropy. *Biochemistry* **39**, 9275–9284
46. Chen, J. C., Krucinski, J., Miercke, L. J., Finer-Moore, J. S., Tang, A. H., Leavitt, A. D., and Stroud, R. M. (2000) Crystal structure of the HIV-1 integrase catalytic core and C-terminal domains: a model for viral DNA binding. *Proc. Natl. Acad. Sci. U.S.A.* **97**, 8233–8238
47. Weeks, S. D., Drinker, M., and Loll, P. J. (2007) Ligation independent cloning vectors for expression of SUMO fusions. *Protein Expr. Purif.* **53**, 40–50
48. Mertens, H. D., and Svergun, D. I. (2010) Structural characterization of proteins and complexes using small-angle X-ray solution scattering. *J. Struct. Biol.* **172**, 128–141
49. Putnam, C. D., Hammel, M., Hura, G. L., and Tainer, J. A. (2007) X-ray solution scattering (SAXS) combined with crystallography and computation: defining accurate macromolecular structures, conformations and assemblies in solution. *Q. Rev. Biophys.* **40**, 191–285
50. Zuo, P., and Manley, J. L. (1993) Functional domains of the human splicing factor ASF/SF2. *EMBO J.* **12**, 4727–4737
51. Colwill, K., Feng, L. L., Yeakley, J. M., Gish, G. D., Cáceres, J. F., Pawson, T., and Fu, X. D. (1996) SRPK1 and Clk/Sty protein kinases show distinct substrate specificities for serine/arginine-rich splicing factors. *J. Biol. Chem.* **271**, 24569–24575
52. Rambo, R. P., and Tainer, J. A. (2013) Accurate assessment of mass, models and resolution by small-angle scattering. *Nature* **496**, 477–481
53. De Houwer, S., Demeulemeester, J., Thys, W., Rocha, S., Dirix, L., Gijssbers, R., Christ, F., and Debyser, Z. (2014) The HIV-1 integrase mutant R263A/K264A is 2-fold defective for TRN-SR2 binding and viral nuclear import. *J. Biol. Chem.* **289**, 25351–25361
54. Larue, R., Gupta, K., Wuensch, C., Shkriabai, N., Kessler, J. J., Danhart, E., Feng, L., Taltynov, O., Christ, F., Van Duynne, G. D., Debyser, Z., Foster, M. P., and Kvaratskhelia, M. (2012) Interaction of the HIV-1 intasome with transportin 3 protein (TNPO3 or TRN-SR2). *J. Biol. Chem.* **287**, 34044–34058
55. Eijkelenboom, A. P., Sprangers, R., Hård, K., Puras Lutzke, R. A., Plasterk, R. H., Boelens, R., and Kaptein, R. (1999) Refined solution structure of the C-terminal DNA-binding domain of human immunovirus-1 integrase. *Proteins* **36**, 556–564
56. Passos, D. O., Li, M., Yang, R., Rebensburg, S. V., Ghirlando, R., Jeon, Y., Shkriabai, N., Kvaratskhelia, M., Craigie, R., and Lyumkis, D. (2017) Cryo-EM structures and atomic model of the HIV-1 strand transfer complex intasome. *Science* **355**, 89–92
57. Hare, S., Gupta, S. S., Valkov, E., Engelman, A., and Cherepanov, P. (2010) Retroviral intasome assembly and inhibition of DNA strand transfer. *Nature* **464**, 232–236
58. Yin, Z., Shi, K., Banerjee, S., Pandey, K. K., Bera, S., Grandgenett, D. P., and Aihara, H. (2016) Crystal structure of the Rous sarcoma virus intasome. *Nature* **530**, 362–366
59. Ballandras-Colas, A., Brown, M., Cook, N. J., Dewdney, T. G., Demeler, B., Cherepanov, P., Lyumkis, D., and Engelman, A. N. (2016) Cryo-EM reveals a novel octameric integrase structure for betaretroviral intasome function. *Nature* **530**, 358–361
60. Ballandras-Colas, A., Maskell, D. P., Serrao, E., Locke, J., Swuec, P., Jónsson, S. R., Kotecha, A., Cook, N. J., Pye, V. E., Taylor, I. A., Andrésdóttir, V., Engelman, A. N., Costa, A., and Cherepanov, P. (2017) A supramolecular assembly mediates lentiviral DNA integration. *Science* **355**, 93–95
61. Studier, F. W. (2005) Protein production by auto-induction in high density shaking cultures. *Protein Expr. Purif.* **41**, 207–234
62. Maertens, G., Cherepanov, P., Pluymers, W., Busschots, K., De Clercq, E., Debyser, Z., and Engelborghs, Y. (2003) LEDGF/p75 is essential for nuclear and chromosomal targeting of HIV-1 integrase in human cells. *J. Biol. Chem.* **278**, 33528–33539
63. Cherepanov, P., Maertens, G., Proost, P., Devreese, B., Van Beeumen, J., Engelborghs, Y., De Clercq, E., and Debyser, Z. (2003) HIV-1 integrase forms stable tetramers and associates with LEDGF/p75 protein in human cells. *J. Biol. Chem.* **278**, 372–381
64. Graewert, M. A., Franke, D., Jeffries, C. M., Blanchet, C. E., Ruskule, D., Kuhle, K., Flieger, A., Schäfer, B., Tartsch, B., Meijers, R., and Svergun, D. I. (2015) Automated pipeline for purification, biophysical and x-ray analysis of biomacromolecular solutions. *Sci. Rep.* **5**, 10734
65. Petoukhov, M. V., Franke, D., Shkumatov, A. V., Tria, G., Kikhney, A. G., Gajda, M., Gorba, C., Mertens, H. D., Konarev, P. V., and Svergun, D. I. (2012) New developments in the ATSAS program package for small-angle scattering data analysis. *J. Appl. Crystallogr.* **45**, 342–350
66. Shkumatov, A. V., and Strelkov, S. V. (2015) DATASW, a tool for HPLC-SAXS data analysis. *Acta Crystallogr. D Biol. Crystallogr.* **71**, 1347–1350

Interaction of TRN-SR2 with HIV integrase

67. Fischer, H., Neto, M. D., Napolitano, H. B., Polikarpov, I., and Craievich, A. F. (2010) Determination of the molecular weight of proteins in solution from a single small-angle X-ray scattering measurement on a relative scale. *J. Appl. Crystallogr.* **43**, 101–109
68. Svergun, D. I. (1999) Restoring low resolution structure of biological macromolecules from solution scattering using simulated annealing. *Biophys. J.* **76**, 2879–2886
69. Franke, D., and Svergun, D. I. (2009) DAMMIF, a program for rapid *ab-initio* shape determination in small-angle scattering. *J. Appl. Crystallogr.* **42**, 342–346
70. Petoukhov, M. V., and Svergun, D. I. (2005) Global rigid body modeling of macromolecular complexes against small-angle scattering data. *Biophys. J.* **89**, 1237–1250
71. Lindahl, E., Azuara, C., Koehl, P., and Delarue, M. (2006) NOMAD-Ref: visualization, deformation and refinement of macromolecular structures based on all-atom normal mode analysis. *Nucleic Acids Res.* **34**, W52–W56
72. Panjkovich, A., and Svergun, D. I. (2016) Deciphering conformational transitions of proteins by small angle X-ray scattering and normal mode analysis. *Phys. Chem. Chem. Phys.* **18**, 5707–5719

N-terminal half of transportin SR2 interacts with HIV integrase
Vicky G. Tsirkone, Jolien Blokken, Flore De Wit, Jolien Breemans, Stéphanie De
Houwer, Zeger Debyser, Frauke Christ and Sergei V. Strelkov

J. Biol. Chem. 2017, 292:9699-9710.

doi: 10.1074/jbc.M117.777029 originally published online March 29, 2017

Access the most updated version of this article at doi: [10.1074/jbc.M117.777029](https://doi.org/10.1074/jbc.M117.777029)

Alerts:

- [When this article is cited](#)
- [When a correction for this article is posted](#)

[Click here](#) to choose from all of JBC's e-mail alerts

This article cites 72 references, 25 of which can be accessed free at
<http://www.jbc.org/content/292/23/9699.full.html#ref-list-1>